Title: Ganglioside synthase knock-out reduces prion disease incubation time in mouse models

Authors: Atsushi Kobayashi,[1*] Zechen Qi,[1] Taishi Shimazaki,[1] Yoshiko Munesue,[1] Tomomi Miyamoto,[2] Norikazu Isoda,[3,4] Hirofumi Sawa,[3,5] Keisuke Aoshima,[1] Takashi Kimura,[1] Shirou Mohri,[6] Tetsuyuki Kitamoto,[6] Tadashi Yamashita,[7] and Ichiro Miyoshi [8]

Affiliations: [1]Laboratory of Comparative Pathology, Faculty of Veterinary Medicine, Hokkaido University, Kita 18 Nishi 9, Kita-ku, Sapporo 060-0818, Japan; [2]Center for Experimental Animal Science, Graduate School of Medical Sciences, Nagoya City University, Mizuho-cho, Mizuho-ku, Nagoya 467-8601, Japan; [3]Global Station for Zoonosis Control, Global Institute for Collaborative Research and Education (GI-CoRE), Hokkaido University; [4]Unit of Risk Analysis and Management, Research Center for Zoonosis Control, Hokkaido University, Kita 20 Nishi 10, Kita-ku, Sapporo 001-0020, Japan; [5]Division of Molecular Pathobiology, Research Center for Zoonosis Control, Hokkaido University, Kita 20 Nishi 10, Kita-ku, Sapporo 001-0020, Japan; [6]Department of Neurological Science, Tohoku University Graduate School of Medicine, 2-1 Seiryo-machi, Aoba-ku, Sendai 980-8575, Japan; [7]Laboratory of Biochemistry, Graduate School of Veterinary Medicine, Azabu University, Sagamihara, Kanagawa 252-5201, Japan; [8]Department of Laboratory Animal Medicine, Tohoku University Graduate School of Medicine, 2-1 Seiryo-machi, Aoba-ku, Sendai 980-8575, Japan.

***Corresponding author:** Atsushi Kobayashi; Laboratory of Comparative Pathology, Faculty of Veterinary Medicine, Hokkaido University, Kita 18 Nishi 9, Kita-ku, Sapporo 060-0818, JAPAN; Tel, +81-11-706-5192; Fax, +81-11-706-5194; E-mail, kobayashi@vetmed.hokudai.ac.jp

Short running title: Gangliosides and prion diseases

Number of text pages: 21

Number of words in abstract: 162

Number of figures (color figures): 6 (4)

Number of tables: 0

Sources of support: Grants-in-Aid for Scientific Research from JSPS (18K05963; A.K.), a grant from The Ichiro Kanehara Foundation (A.K.), a grant from The Suhara Memorial Foundation (A.K.), and a grant from The Kato Memorial Trust for Nambyo Research (A.K.).

Disclosures: None declared.

ABSTRACT

Localization of the abnormal and normal isoforms of prion proteins to detergent-resistant membrane microdomains, lipid rafts, is considered to be important for the conformational conversion. Lipid rafts are enriched in sialic acid-containing glycosphingolipids, namely gangliosides. Alteration in the ganglioside composition of lipid rafts can affect the localization of lipid raft-associated proteins. To investigate the role of gangliosides in the pathogenesis of prion diseases, we performed intracerebral transmission study of a scrapie prion strain Chandler and a Gerstmann-Sträussler-Scheinker syndrome prion strain Fukuoka-1 using various knock-out mouse lines ablated with ganglioside synthase gene, *i.e.*, GD2/GM2 synthase, GD3 synthase, or GM3 synthase. Following challenge with the Chandler strain, GD2/GM2 synthase knock-out mice showed 20% reduction of incubation time, reduced prion protein deposition in the brain with attenuated glial reactions, and reduced localization of prion proteins to lipid rafts. These results raise the possibility that the gangliosides may have an important role in prion disease pathogenesis by affecting the localization of prion proteins to lipid rafts.

INTRODUCTION

Prion diseases are fatal transmissible neurodegenerative diseases including Creutzfeldt-Jakob disease (CJD), Gerstmann-Sträussler-Scheinker syndrome, and fatal familial insomnia in humans, or bovine spongiform encephalopathy, chronic wasting disease, and scrapie in animals. Accumulation of an abnormal protease-resistant isoform of prion protein (PrP^{Sc}), which is generated by conformational conversion of the normal cellular isoform (PrP^{C}), is one of the pathognomonic features of prion diseases (1).

Membrane microdomains where PrP^{C} and PrP^{Sc} localized are lipid rafts (2-6). Lipid rafts are enriched in cholesterol, sphingolipids, and glycosylphosphatidylinositol (GPI)-anchored proteins including PrP, and show partial resistance against mild detergent treatment (7, 8). Therefore, lipid rafts buoy toward low density fractions in density gradient ultracentrifugation after mild detergent treatment, namely flotation assay. Lipid rafts have been reported to serve many microorganisms for infection or serve the clustering of receptors or signaling molecules to facilitate signal transduction (8, 9). In prion disease pathogenesis, the localization of PrP^{C} and PrP^{Sc} to lipid rafts has been reported to be important for the conformational conversion (3).

Gangliosides are sialic acid-containing glycosphingolipids highly expressed in the brain. Gangliosides are synthesized in the Golgi apparatus by specific glycosyltransferases, the expression of which controls the steady-state levels of gangliosides (10). Gangliosides are characterized by the number and positions of sialic acids that define their classification into A, M, D, T, Q, and P (zero to five sialic acids) and a, b, and c series (one, two, or three sialic acids on internal galactose residue) (Figure 1). Gangliosides are embedded in the outer layer of the plasma membrane and one of major components of lipid rafts (7). Therefore, alteration in the ganglioside composition of lipid rafts can affect the localization of lipid raft-associated proteins (11-13). For example, knock-out (KO) mice lacking GD2/GM2 synthase, in which GA2, GM2, GD2, GT2,

and downstream gangliosides are depleted, show the dispersion of lipid raft-associated proteins such as caveolin 1 or flotillin 1 from lipid raft fractions in flotation assay (13). Furthermore, in KO mice lacking both GD2/GM2 synthase and GD3 synthase, a GPI-anchored complement-regulatory protein CD55/decay-accelerating factor also disperses from lipid rafts, and unfavorable activation of complement system occurs (12). Complement activation starts with the activation of C1q by antigen-antibody complex or spontaneous hydrolysis of C3 and causes a cascade of further cleavage and activation processes of complement proteins. Complement activation results in the accumulation of complement proteins such as C1q or C3b and the formation of the membrane attack complex. In the KO mice lacking both GD2/GM2 synthase and GD3 synthase, gene expression of complement proteins such as C1qa, C3, or C4 was up-regulated, and deposition of C1q in the brain increased (12, 13). Meanwhile, an activation of the complement system and accumulation of C1q, C3, or membrane attack complex have also been demonstrated in brains of human patients with prion diseases or prion-infected animals (14, 15). The role of complement activation in prion disease pathogenesis has been proposed to cause degeneration of prion-infected neurons or to facilitate microglial phagocytosis of prion-infected neurons (15).

In this study, we performed a prion transmission study using various ganglioside synthase knock-out mouse lines to investigate the role of gangliosides in the pathogenesis of prion diseases.

MATERIALS AND METHODS

Ethics statement

Animal experiments were performed in strict accordance with the Regulations for Animal Experiments and Related Activities at Hokkaido University and Fundamental Guidelines for Proper Conduct of Animal Experiment and Related Activities in Academic Research Institutions by Ministry of Education, Culture, Sports, Science and Technology in Japan, Notice No. 71. The

protocol was approved by the Institutional Animal Care and Use Committees of Hokkaido University (14-0170).

Mice

Generation of KO mice lacking GD2/GM2 synthase (B4GALNT1), GD3 synthase (ST8SIA1), or GM3 synthase (ST3GAL5) have been reported previously (16, 17). These mice were backcrossed to C57BL/6, and the resulting heterozygous animals were intercrossed to provide homozygous KO mice and wild-type (WT) littermate controls. Thus, all of the KO mice and WT littermate controls were on a C57BL/6 background.

Sources of inocula

A mouse-adapted scrapie prion strain Chandler (18) was kindly provided by Dr. Motohiro Horiuchi. A mouse-adapted Gerstmann-Sträussler-Scheinker syndrome prion strain Fukuoka-1 (19) was maintained in C57BL/6 mice. The inocula were prepared from the brain of terminally ill mice.

Transmission experiments

Intracerebral inoculation was performed as described (20). Briefly, 10% brain homogenates were prepared in sterile phosphate-buffered saline using glass homogenizers, and 20 μl of the homogenates were intracerebrally inoculated into mice (n = 6 or 7). The inoculated mice were sacrificed at a predefined clinical endpoint, or at the time point showing intercurrent illness. One hemisphere of the brain was fixed in 10% buffered formalin for histopathological analysis, and the other hemisphere was immediately frozen for biochemical analysis.

Immunohistochemistry

Formalin-fixed mouse brain tissues were treated with 60% formic acid for 1 hour to inactivate the infectivity and embedded in paraffin. The embedded tissues were sectioned at a thickness of 5 μm. Tissue sections were pretreated by hydrolytic autoclaving before PrP immunohistochemistry (21). The anti-PrP antiserum PrP-N (22), rabbit anti-ionized calcium-binding adapter molecule 1 (Iba1) polyclonal antibody (FUJIFILM Wako Pure Chemical Corporation, Osaka, Japan), and rabbit anti-glial fibrillary acidic protein (GFAP) polyclonal antibody (Dako, Glostrup, Denmark) were used as the primary antibodies. Goat-anti-rabbit immunoglobulin polyclonal antibody labelled with the peroxidase-conjugated dextran polymer, EnVision^{+} (Dako) was used as the secondary antibody. For routine histopathological analysis, the tissue sections were also stained with hematoxylin and eosin (H&E).

PrP^{Sc} purification

PrP^{Sc} was purified from the mouse brain as described (23). Briefly, brain tissues were homogenized in 2 ml of lysis buffer (100 mM Tris-HCl pH 8.0, 10 mM NaCl, 10 mM $MgCl_2$, 2% Triton X-100, and 25 units/ml DNase I (Takara Bio, Shiga, Japan)) and digested with collagenase (1 mg/200 mg tissue) (FUJIFILM Wako Pure Chemical Corporation) overnight at room temperature. Collagenase digestion disrupts the connective tissue and improves the accessibility of detergents and/or proteinase K (PK) to PrP^{Sc} (24). The digested homogenates were ultracentrifuged at 453,000 *g* for 30 min at 4°C, and the pellets were resuspended and sonicated in 870 μl of PK-digestion buffer (100 mM Tris-HCl pH 8.0 and 5% Sarkosyl (Sigma-Aldrich, St. Louis, MO)). The resuspended samples were centrifuged at 10,000 *g* for 3 min to remove the cell debris, and the supernatants (800 μl) were digested with PK (4 μg/200 mg tissue) (FUJIFILM Wako Pure Chemical Corporation) for 1 h at 37°C. It has been reported that these conditions for

PK-digestion were sufficient for the complete digestion of normal PrP^{C}, and that higher PK concentrations caused unfavorable degradation of PrP^{Sc} (25). The PK-digested proteins were precipitated by adding 200 µl of 99.5% ethanol and ultracentrifugation at 135,000 *g* for 30 min at 4°C. The pellets were resuspended in 400 µl/200 mg tissue of Laemmli's sample buffer (60 mM Tris-HCl pH 6.8, 5% glycerol, 2% SDS, and 0.01% bromophenol blue) and boiled at 100°C for 5 min. To examine the expression level of PrP^{C}, C1qa, and β-actin, 10% homogenates were prepared from uninfected mouse brains using the lysis buffer. The homogenates were boiled with the addition of 0.25×volume of 5×Laemmli's sample buffer.

Flotation assay

To isolate lipid rafts, a flotation assay was performed as described previously (26). Briefly, 10% homogenates were prepared from uninfected mouse brains using citrate buffer (20 mM sodium citrate and 137 mM NaCl (pH 6.0)). The homogenates were centrifuged at 1,000 *g* for 5 min at 4°C to remove cell debris and nuclei. The supernatants were mixed with 1×volume of ice-cold Brij O-10 extraction buffer (0.1% Brij O-10 (Sigma-Aldrich), 20 mM sodium citrate, and 137 mM NaCl (pH 6.0)) and incubated on a rocker at 4°C for 30 min, and then mixed with 1.4×volume of 60% Optiprep (Axis-Shield, Dundee, UK). In 12 ml polycarbonate centrifuge tubes (Beckman Coulter, Brea, CA), 9 ml of 0-30% Optiprep continuous gradients were prepared by Gradient Master (BioComp Instruments, Fredericton, NB, Canada) according to the manufacturer's instruction and underlaid with 2 ml of the Brij O-10 extracted samples. The gradients were centrifuged in a pre-chilled Beckman SW41 rotor (Beckman Coulter) at 40,000 *g* for 130 min at 4°C. The samples were split to 18 fractions (600 µl each) from top (fraction 1) to bottom (fraction 18) and boiled with the addition of 150 µl of 5×Laemmli's sample buffer.

Western blotting

Protein samples were subjected to SDS-PAGE using 13.5% Tris-glycine long gels of 15 cm length and western blotting as described (27). The anti-PrP monoclonal antibody SAF83 (Bertin Bioreagents, Montigny le Bretonneux, France), anti-β-actin monoclonal antibody 2F3 (FUJIFILM Wako Pure Chemical Corporation), anti-flotillin 1 monoclonal antibody 18/Flotillin-1 (BD Biosciences, San Jose, CA), anti-C1qa polyclonal antibody (Abcam, Cambridge, UK), anti-CD55 monoclonal antibody #583905 (R&D systems, Minneapolis, MN), anti-voltage-gated calcium channel auxiliary subunit α2δ-1 (CACNA2D1) monoclonal antibody 20A (Abcam), and anti-Thy1.2 monoclonal antibody (Bio-Rad, Hercules, CA) were used as the primary antibodies. The anti-mouse EnVision+ (Dako), anti-rabbit EnVision+ (Dako), and ECL anti-rat IgG antibody (GE Healthcare, Chicago, IL) were used as the secondary antibodies. The blots were visualized with Luminata Forte Western HRP substrate (MilliporeSigma, Burlington, MA), and images were obtained by imaging device ImageQuant LAS 4000 mini (GE Healthcare). The signal intensities of the western blots were quantified with ImageQuant TL software (GE Healthcare).

Image analysis

Severity of spongiform change was classified into three scores: 1, negative/mild (approximately 0-20% of the tissue section showed spongiform change); 2, moderate (approximately 20-60%); 3, severe (approximately 60-100%). Immunohistochemical staining intensities were classified into three scores: 1, negative/weak (approximately 0-20% of the tissue section showed immunoreactivity); 2, moderate (approximately 20-60%); and 3, high (approximately 60-100%). Cerebral cortex, cerebellar cortex, striatum, thalamus, hippocampus, pons and cerebellar white matter sections were used for the scoring of spongiform change, and cerebral cortex sections were used for the scoring of immunohistochemistry. Scoring was performed independently by two

pathologists in a blinded manner, and the scores were finalized after discussion. Data were collected from all diseased mice and are represented as mean±SEM in the scoring of spongiform change or as % of animals with each score in the scoring of immunohistochemistry.

Statistical analysis

The Kaplan-Meier log-rank test was used to analyze survival data in transmission study. Tukey-Kramer test was used to analyze signal intensity data in western blot analysis. The statistical tests were carried out using the statistical software EZR, version 1.36 (28). $P < 0.05$ was considered statistically significant.

RESULTS

Transmission of prions to KO mice lacking ganglioside synthase gene

To investigate the role of gangliosides in the pathogenesis of prion diseases, we performed intracerebral transmission study using KO mice lacking GD2/GM2 synthase (GD2/GM2 KO), GD3 synthase (GD3 KO), or GM3 synthase (GM3 KO). These KO mice lack particular ganglioside species depending on the ablated ganglioside synthase gene (Figure 1). For a mouse-adapted scrapie strain Chandler, the mean incubation time of GD2/GM2 KO mice (126.6±0.3 days) was reduced by 20% compared with that of WT mice (157.5±1.2 days, $P < 0.01$) (Figure 2). The mean incubation time of GM3 KO mice was also slightly reduced (149.5±2.2 days, $P < 0.01$). For a mouse-adapted Gerstmann-Sträussler-Scheinker syndrome strain Fukuoka-1, the mean incubation time of GD2/GM2 KO mice and GM3 KO mice tended to be reduced compared with that of WT mice, though the differences were not statistically significant.

Neuropathology

Prion strains are characterized by neuropathological features and biochemical properties of PrP^{Sc} in the inoculated mice. Therefore, we next performed neuropathological analysis of the inoculated mice to examine whether the strain characteristics were altered by the ablation of the ganglioside synthase gene. In the Chandler-inoculated mice, spongiform changes were distributed through the cerebral and cerebellar cortices, striatum, thalamus, hippocampus, pons, and cerebellar white matter (Figure 3A). In the Fukuoka-1-inoculated mice, the vacuoles of spongiform changes became larger and were distributed more intensively in the pons and cerebellar white matter (Figure 3B, C). There was no difference in the distribution of spongiform changes among mouse lines (Figure 3C). However, in immunohistochemical analysis of disease-associated PrP, PrP^{TSE}, GD2/GM2 KO mice inoculated with the Chandler strain showed decreased PrP^{TSE} deposition (Figures 3A, D). In addition, Iba1-positive microglia and GFAP-positive astroglia were also fewer in the Chandler-inoculated GD2/GM2 KO mice. For the Fukuoka-1 strain, GD2/GM2 KO mice showed decreased microglial reaction, but PrP^{TSE} deposition or astroglial reaction was not altered (Figures 3B, D).

Biochemical properties of PrP^{Sc}

Western blot analysis of PK-resistant PrP^{Sc} in the brain revealed that the strain-specific biochemical properties of PrP^{Sc}, *i.e.*, apparent molecular mass and patterns of *N*-linked glycosylation, were not modified by the absence of ganglioside synthase genes (Figure 4A). The apparent molecular mass of PrP^{Sc} in the Chandler-inoculated mice was smaller than that in the Fukuoka-1-inoculated mice, regardless of the mouse genotype. Meanwhile, the Chandler-inoculated GD2/GM2 KO mice showed slightly decreased PrP^{Sc} accumulation compared with WT, GD3 KO, or GM3 KO mice (Figure 4A, B). Of note, the apparent amount of PrP^{Sc} in western blot analysis did not reflect the degree of PrP^{TSE} deposition in the immunohistochemical analysis.

For example, a GD2/GM2 KO mouse (#145) that showed reduced PrP^{TSE} deposition in the immunohistochemical analysis, *i.e.*, score 1, had similar apparent amount of PrP^{Sc} to that of another GD2/GM2 KO mouse (#203) that showed abundant PrP^{TSE} deposition in the immunohistochemistry, *i.e.*, score 3 (Figure 4A). Thus, GD2/GM2 KO showed shortened incubation time, reduced PrP^{TSE} deposition with attenuated glial reactions in neuropathological analysis, and slightly decreased PK-resistant PrP^{Sc} accumulation in western blot analysis.

In addition, we compared the amount of PrP^{C} in the brain of uninfected KO mice because the expression level of PrP^{C} can directly affect the incubation period. However, the amount of PrP^{C} was not modified by the absence of ganglioside synthase genes (Figure 4C), suggesting that the expression level of PrP^{C} is unrelated to the changes in incubation period.

Evaluation of complement system

To gain insights into the shortened incubation period in GD2/GM2 KO mice, we then examined the involvement of complement system because it has been reported that KO mice lacking both GD2/GM2 synthase and GD3 synthase show dispersion of GPI-anchored complement-regulatory proteins from lipid rafts and activation of the complement system (12, 13). To assess the activation of the complement system, the amount of a complement factor C1qa in the brain was compared between GD2/GM2 KO mice and WT mice by western blot analysis (Figure 5). However, there was no difference in C1qa level between GD2/GM2 KO mice and WT mice. C1qa accumulated only in the prion-infected animals regardless of the mouse genotype or prion strain. In addition, although dispersion of GPI-anchored complement-regulatory protein CD55 from lipid rafts has been demonstrated in KO mice lacking both GD2/GM2 synthase and GD3 synthase, the floating patterns of CD55 were not different between GD2/GM2 KO mice and WT mice in the flotation assay of lipid raft-associated proteins in the brain (Figure 6A), suggesting that CD55 did not

disperse from lipid rafts in GD2/GM2 KO mice. Thus, the shortened incubation period in the Chandler-inoculated GD2/GM2 KO mice was not due to altered activation of the complement system.

Flotation assay of PrP^C and lipid raft-associated proteins

We subsequently investigated whether PrP^C and lipid raft-associated proteins other than CD55 disperse from lipid rafts in GD2/GM2 KO mice by flotation assay. As reported previously (13), a lipid raft marker flotillin 1 dispersed from the lipid raft fractions (fractions 7-11) to the non-raft fractions (fractions 15-18) in GD2/GM2 KO mice (Figure 6B). Furthermore, PrP^C also dispersed from the lipid raft fractions to the non-raft fractions in GD2/GM2 KO mice (Figure 6C). In contrast, the floating patterns of a GPI-anchored PrP-associated calcium channel protein CACNA2D1 (29,30) or those of a GPI-anchored protein Thy1 were not different between GD2/GM2 KO mice and WT mice (Figure 6D, E). Thus, certain lipid raft-associated proteins including PrP^C dispersed from lipid rafts in the brain of GD2/GM2 KO mice.

DISCUSSION

Here we found that GD2/GM2 KO mice inoculated with the Chandler prion strain showed shortened incubation time, reduced PrP^{TSE} deposition with attenuated glial reactions in neuropathological analysis, slightly decreased PK-resistant PrP^{Sc} accumulation in western blot analysis, and reduced localization of PrP to lipid rafts.

The reduced localization of PrP to lipid rafts might affect the formation of PrP^{Sc} in GD2/GM2 KO mice. Although the localization of PrP^{Sc} to lipid rafts could not be examined, dispersion of lipid raft-associated proteins including PrP^C from lipid rafts was confirmed in GD2/GM2 KO mice in the present study. Since the localization to lipid rafts is important for the conformational

conversion of PrP^{C} into PrP^{Sc} (3), the dispersion of PrP^{C} and/or PrP^{Sc} from lipid rafts might result in the decreased accumulation of PrP^{TSE} and PK-resistant PrP^{Sc} in the Chandler-inoculated GD2/GM2 KO mice. It is noteworthy that the amount of PK-resistant PrP^{Sc} in the Chandler-inoculated GD2/GM2 KO mice in the western blot analysis did not reflect the marked reduction of PrP^{TSE} deposition in the immunohistochemical analysis compared with the other mouse lines. In addition, even in the Chandler-inoculated GD2/GM2 KO mouse group, the apparent amount of PK-resistant PrP^{Sc} did not reflect the PrP^{TSE} deposition score in the immunohistochecmical analysis. This finding raises a possibility that the amount of PK-sensitive PrP^{Sc} (31-33) might largely decrease in the Chandler-inoculated GD2/GM2 KO mice. Meanwhile, the incubation time was shortened in the Chandler-inoculated GD2/GM2 KO mice in spite of the decreased PrP^{Sc} accumulation. To account for this discrepancy, further studies will be needed in the future addressing the questions whether the dispersion of PrP^{Sc} and/or PrP^{C} from lipid rafts reduces the formation of PK-sensitive PrP^{Sc} or affects the neurotoxicity of PrP^{Sc}.

There remains a possibility that the alteration in ganglioside composition might directly affect the conformation of PrP. The ablation of ganglioside synthase causes massive alteration of ganglioside composition (17). For example, an ablation of GD2/GM2 synthase causes depletion of GD2, GM2 and downstream gangliosides such as GM1, and results in accumulation of GD3 and GM3 (16, 34). PrP^{C} is co-localized and co-immunoprecipitated with GM1 and GM3 (35, 36). GM1 binds to the C-terminus of PrP and modifies the conformational properties of PrP (37, 38). Similarly, GM1 binds to amyloid β (Aβ) and modifies the conformation of Aβ, resulting in the formation of endogenous seeds for amyloid fibril formation (39). Therefore, the direct effects of gangliosides on PrP conformation are not negligible. To test this hypothesis, analysis of conformational properties of PrP^{C} and PrP^{Sc} from GD2/GM2 KO mice will be needed in the future.

We cannot exclude a possibility that the alteration in ganglioside composition might affect the

activation of glial cells. Although the role of glial cells in the pathogenesis of prion diseases is controversial, both microglia and astroglia are activated in prion diseases (40-43). The decreased number of microglia and astroglia in the Chandler-inoculated GD2/GM2 KO mice might simply reflect the decreased PrP^{TSE} deposition. However, although the amount of PrP^{TSE} deposition was not altered, the Fukuoka-1-inoculated GD2/GM2 KO mice also showed attenuated microglial reaction. Therefore, the altered ganglioside composition may affect glial reactions regardless of the PrP^{TSE} accumulation. Indeed, ethanol-induced astroglial activation is attenuated in GD2/GM2 KO mice (44). Further studies will be required to examine whether the shortened incubation time in GD2/GM2 KO mice relates to the attenuated microglial reaction including neuroprotective microglia (45, 46).

In conclusion, we have shown that the ablation of GD2/GM2 synthase gene causes a significant reduction in incubation time of prion infection. The present study suggests that the gangliosides may have an important role in prion disease pathogenesis by affecting the localization of PrP to lipid rafts.

ACKNOWLEDGMENTS

We thank Drs. Motohiro Horiuchi and Takeshi Yamasaki (Faculty of of Veterinary Medicine, Hokkaido University) for providing us with the prion inoculum and technical assistance.

REFERENCES

1. Prusiner SB, Scott MR, DeArmond SJ, Cohen FE: Prion protein biology. Cell 1998, 93:337–348.

2. Harmey JH, Doyle D, Brown V, Rogers MS: The cellular isoform of the prion protein, PrPc, is associated with caveolae in mouse neuroblastoma (N2a) cells. Biochem Biophys Res Commun 1995, 210:753-759.
3. Taraboulos A, Scott M, Semenov A, Avrahami D, Laszlo L, Prusiner SB: Cholesterol depletion and modification of COOH-terminal targeting sequence of the prion protein inhibit formation of the scrapie isoform. J Cell Biol 1995, 129:121-132.
4. Vey M, Pilkuhn S, Wille H, Nixon R, DeArmond SJ, Smart EJ, Anderson RG, Taraboulos A, Prusiner SB: Subcellular colocalization of the cellular and scrapie prion proteins in caveolae-like membranous domains. Proc Natl Acad Sci USA 1996, 93:14945-14949.
5. Naslavsky N, Stein R, Yanai A, Friedlander G, Taraboulos A: Characterization of detergent-insoluble complexes containing the cellular prion protein and its scrapie isoform. J Biol Chem 1997, 272:6324-6331.
6. Naslavsky N, Shmeeda H, Friedlander G, Yanai A, Futerman AH, Barenholz Y, Taraboulos A: Sphingolipid depletion increases formation of the scrapie prion protein in neuroblastoma cells infected with prions. J Biol Chem 1999, 274:20763-20771.
7. Brown DA, Rose JK: Sorting of GPI-anchored proteins to glycolipid-enriched membrane subdomains during transport to the apical cell surface. Cell 1992, 68:533-544.
8. Simons K, Ikonen E: Functional rafts in cell membranes. Nature 1997, 387:569-572.
9. Bollinger CR, Teichgräber V, Gulbins E: Ceramide-enriched membrane domains. Biochim Biophys Acta 2005, 1746:284-294.
10. Groux-Degroote S, Guérardel Y, Delannoy P: Gangliosides: Structures, Biosynthesis, Analysis, and Roles in Cancer. Chembiochem. 2017, 18:1146-1154.

11. Kabayama K, Sato T, Kitamura F, Uemura S, Kang BW, Igarashi Y, Inokuchi J: TNFalpha-induced insulin resistance in adipocytes as a membrane microdomain disorder: involvement of ganglioside GM3. Glycobiology 2005, 15:21-29.
12. Ohmi Y, Tajima O, Ohkawa Y, Mori A, Sugiura Y, Furukawa K, Furukawa K: Gangliosides play pivotal roles in the regulation of complement systems and in the maintenance of integrity in nerve tissues. Proc Natl Acad Sci USA 2009, 106:22405-22410.
13. Ohmi Y, Tajima O, Ohkawa Y, Yamauchi Y, Sugiura Y, Furukawa K, Furukawa K: Gangliosides are essential in the protection of inflammation and neurodegeneration via maintenance of lipid rafts: elucidation by a series of ganglioside-deficient mutant mice. J Neurochem 2011, 116:926-935.
14. Kovacs GG, Gasque P, Ströbel T, Lindeck-Pozza E, Strohschneider M, Ironside JW, Budka H, Guentchev M: Complement activation in human prion disease. Neurobiol Dis 2004, 15:21-28.
15. Hasebe R, Raymond GJ, Horiuchi M, Caughey B: Reaction of complement factors varies with prion strains in vitro and in vivo. Virology 2012, 423:205-213.
16. Liu Y, Wada R, Kawai H, Sango K, Deng C, Tai T, McDonald MP, Araujo K, Crawley JN, Bierfreund U, Sandhoff K, Suzuki K, Proia RL: A genetic model of substrate deprivation therapy for a glycosphingolipid storage disorder. J Clin Invest 1999, 103:497-505.
17. Yamashita T, Hashiramoto A, Haluzik M, Mizukami H, Beck S, Norton A, Kono M, Tsuji S, Daniotti JL, Werth N, Sandhoff R, Sandhoff K, Proia RL: Enhanced insulin sensitivity in mice lacking ganglioside GM3. Proc Natl Acad Sci USA 2003, 100:3445-3449.
18. Chandler RL: Encephalopathy in mice produced by inoculation with scrapie brain material. 1961, Lancet 1:1378-1379.

19. Tateishi J, Ohta M, Koga M, Sato Y, Kuroiwa Y: Transmission of chronic spongiform encephalopathy with kuru plaques from humans to small rodents. Ann Neurol 1979, 5:581-584.
20. Kitamoto T, Mohri S, Ironside JW, Miyoshi I, Tanaka T, Kitamoto N, Itohara S, Kasai N, Katsuki M, Higuchi J, Muramoto T, Shin RW: Follicular dendritic cell of the knock-in mouse provides a new bioassay for human prions. Biochem Biophys Res Commun 2002, 294:280-286.
21. Kitamoto T, Shin RW, Doh-ura K, Tomokane N, Miyazono M, Muramoto T, Tateishi J: Abnormal isoform of prion proteins accumulates in the synaptic structures of the central nervous system in patients with Creutzfeldt-Jakob disease. Am J Pathol 1992, 140:1285-1294.
22. Kitamoto T, Muramoto T, Hilbich C, Beyreuther K, Tateishi J: N-terminal sequence of prion protein is also integrated into kuru plaques in patients with Gerstmann-Sträussler syndrome. Brain Res 1991, 545:319-321.
23. Munesue Y, Shimazaki T, Qi Z, Isoda N, Sawa H, Aoshima K, Kimura T, Mohri S, Kitamoto T, Kobayashi A: Development of a quick bioassay for the evaluation of transmission properties of acquired prion diseases. Neurosci Lett 2018, 668:43-47.
24. Grathwohl KU, Horiuchi M, Ishiguro N, Shinagawa M: Improvement of PrP^{Sc}-detection in mouse spleen early at the preclinical stage of scrapie with collagenase-completed tissue homogenization and Sarkosyl-NaCl extraction of PrP^{Sc}. Arch Virol 1996, 141:1863-1874.
25. Hizume M, Kobayashi A, Teruya K, Ohashi H, Ironside JW, Mohri S, Kitamoto T: Human prion protein (PrP) 219K is converted to PrP^{Sc} but shows heterozygous inhibition in variant Creutzfeldt-Jakob disease infection. J Biol Chem 2009, 284:3603-3609.

26. Baron GS, Hughson AG, Raymond GJ, Offerdahl DK, Barton KA, Raymond LD, Dorward DW, Caughey B: Effect of glycans and the glycophosphatidylinositol anchor on strain dependent conformations of scrapie prion protein: improved purifications and infrared spectra. Biochemistry 2011, 50:4479-4490.
27. Asano M, Mohri S, Ironside JW, Ito M, Tamaoki N, Kitamoto T: vCJD prion acquires altered virulence through trans-species infection. Biochem Biophys Res Commun 2006, 342:293-299.
28. Kanda Y: Investigation of the freely available easy-to-use software'EZR' for medical statistics. Bone Marrow Transplant 2013, 48:452-458.
29. Senatore A, Colleoni S, Verderio C, Restelli E, Morini R, Condliffe SB, Bertani I, Mantovani S, Canovi M, Micotti E, Forloni G, Dolphin AC, Matteoli M, Gobbi M, Chiesa R: Mutant PrP suppresses glutamatergic neurotransmission in cerebellar granule neurons by impairing membrane delivery of VGCC α(2)δ-1 Subunit. Neuron 2012, 74:300-313.
30. Alvarez-Laviada A, Kadurin I, Senatore A, Chiesa R, Dolphin AC: The inhibition of functional expression of calcium channels by prion protein demonstrates competition with α2δ for GPI-anchoring pathways. Biochem J 2014, 458:365-374.
31. Safar J, Wille H, Itri V, Groth D, Serban H, Torchia M, Cohen FE, Prusiner SB: Eight prion strains have PrP(Sc) molecules with different conformations. Nat Med 1998, 4:1157-1165.
32. Tzaban S, Friedlander G, Schonberger O, Horonchik L, Yedidia Y, Shaked G, Gabizon R, Taraboulos A: Protease-sensitive scrapie prion protein in aggregates of heterogeneous sizes. Biochemistry 2002, 41:12868-12875.
33. Safar JG, Geschwind MD, Deering C, Didorenko S, Sattavat M, Sanchez H, Serban A, Vey M, Baron H, Giles K, Miller BL, Dearmond SJ, Prusiner SB: Diagnosis of human prion disease. Proc Natl Acad Sci USA 2005, 102:3501-3506.

34. Takamiya K, Yamamoto A, Furukawa K, Yamashiro S, Shin M, Okada M, Fukumoto S, Haraguchi M, Takeda N, Fujimura K, Sakae M, Kishikawa M, Shiku H, Furukawa K, Aizawa S: Mice with disrupted GM2/GD2 synthase gene lack complex gangliosides but exhibit only subtle defects in their nervous system. Proc Natl Acad Sci USA 1996, 93:10662-10667.
35. Mattei V, Garofalo T, Misasi R, Gizzi C, Mascellino MT, Dolo V, Pontieri GM, Sorice M, Pavan A: Association of cellular prion protein with gangliosides in plasma membrane microdomains of neural and lymphocytic cells. Neurochem Res 2002, 27:743-749.
36. Mattei V, Garofalo T, Misasi R, Circella A, Manganelli V, Lucania G, Pavan A, Sorice M Prion protein is a component of the multimolecular signaling complex involved in T cell activation. FEBS Lett 2004, 560:14-18.
37. Sanghera N, Correia BE, Correia JR, Ludwig C, Agarwal S, Nakamura HK, Kuwata K, Samain E, Gill AC, Bonev BB, Pinheiro TJ: Deciphering the molecular details for the binding of the prion protein to main ganglioside GM1 of neuronal membranes. Chem Biol 2011, 18:1422-1431.
38. Botto L, Cunati D, Coco S, Sesana S, Bulbarelli A, Biasini E, Colombo L, Negro A, Chiesa R, Masserini M, Palestini P: Role of lipid rafts and GM1 in the segregation and processing of prion protein. PLoS One 2014, 9:e98344.
39. Yanagisawa K: GM1 ganglioside and Alzheimer's disease. Glycoconj J 2015, 32:87-91.
40. Miyazono M, Iwaki T, Kitamoto T, Kaneko Y, Doh-ura K, Tateishi J: A comparative immunohistochemical study of Kuru and senile plaques with a special reference to glial reactions at various stages of amyloid plaque formation. Am J Pathol 1991, 139:589-598.
41. Williams A, Lucassen PJ, Ritchie D, Bruce M: PrP deposition, microglial activation, and neuronal apoptosis in murine scrapie. Exp Neurol 1997, 144:433-438.
42. Aguzzi A, Liu Y: A role for astroglia in prion diseases. J Exp Med 2017, 214:3477-3479.

455 43. Aguzzi A, Zhu C: Microglia in prion diseases. J Clin Invest 2017, 127:3230-3239.
456 44. Saito M, Wu G, Hui M, Masiello K, Dobrenis K, Ledeen RW, Saito M: Ganglioside
457 accumulation in activated glia in the developing brain: comparison between WT and
458 GalNAcT KO mice. J Lipid Res 2015, 56:1434-1448.
459 45. Zhu C, Herrmann US, Falsig J, Abakumova I, Nuvolone M, Schwarz P, Frauenknecht K,
460 Rushing EJ, Aguzzi A: A neuroprotective role for microglia in prion diseases. J Exp Med
461 2016, 213:1047-1059.
462 46. Carroll JA, Race B, Williams K, Striebel J, Chesebro B: Microglia Are Critical in Host
463 Defense Against Prion Disease. J Virol 2018, doi: 10.1128/JVI.00549-18.
464

FIGURE LEGENDS

Figure 1. Biosynthetic pathway of gangliosides and elimination of particular gangliosides in KO mouse lines. GD2/GM2, GM3, and GD3 KO mice lack gangliosides circled by red, blue, and magenta line, respectively.

Figure 2. Kaplan-Meier survival curves. Intracerebral transmission of Chandler strain (**A**) or Fukuoka-1 strain (**B**) to each KO mouse line or WT littermate controls. Data are represented as % of surviving animals (y-axis) plotted against the number of days post inoculation (x-axis).

Figure 3. Neuropathological features. (**A**) Histopathological analysis of spongiform changes in H&E stained sections and immunohistochemical analysis for PrP^{TSE} deposition, Iba1-positive microglia, and GFAP-positive astroglia in the cerebral cortices of the Chandler strain-inoculated mice. GD2/GM2 KO mice showed less PrP^{TSE} deposition in the neuropil and attenuated microglial and astroglial reactions. Scale bars: 50 μm. Data are representative of tissue sections from six mice per group. (**B**) Histopathological analysis of the Fukuoka-1 strain-inoculated mice. (**C**) Regional distribution of spongiform change in the brain. Spongiform change was scored on a scale of 1-3: 1, negative/mild (approximately 0-20% of the tissue section showed spongiform change); 2, moderate (approximately 20-60%); 3, severe (approximately 60-100%). Data are represented as mean ± SEM (n = 6). (**D**) Scoring of the immunohistochemical signal intensities. The signal intensities were classified into three scores: 1, negative/weak (approximately 0-20% of the tissue section showed immunoreactivity); 2, moderate (approximately 20-60%); and 3, high (approximately 60-100%). Data are represented as % of animals with each score. The scoring was performed by two pathologists independently, based on the signal intensities in the cerebral cortices.

Figure 4. Western blot analysis of PrP. (**A**) PK-resistant PrP^{Sc} in the brain of Chandler- or Fukuoka-1-inoculated mice. There was no difference in the biochemical properties of PK-resistant PrP^{Sc} among mouse lines. The Chandler-inoculated mice consistently produced lower apparent molecular mass of unglycosylated PrP^{Sc} fragments compared with those of the Fukuoka-1-inoculated mice regardless of their genotype. The Chandler-inoculated GD2/GM2 KO mice showed slightly decreased apparent amount of PrP^{Sc} compared with WT, GD3 KO, or GM3 KO mice, irrespective of the degree of PrP^{TSE} deposition in the immunohistochemical analysis. For example, a GD2/GM2 KO mouse (#145) that showed reduced PrP^{TSE} deposition in the immunohistochemical analysis, *i.e.*, score 1, had similar apparent amount of PK-resistant PrP^{Sc} compared with that of another GD2/GM2 KO mouse (#203) that showed abundant PrP^{TSE} deposition in the immunohistochemistry, *i.e.*, score 3. A brain sample, equivalent to 125 μg in wet weight, was loaded in each lane. (**B**) Quantification of the amount of PK-resistant PrP^{Sc} in the brain of the Chandler-inoculated mice. GD2/GM2 KO mice showed reduced PrP^{Sc} accumulation compared with GD3 KO mice or GM3 KO mice. The mean signal intensity of PrP^{Sc} in GD2/GM2 KO mice was assigned as 100. Data are represented as mean ± SEM (n = 4 or 5). Statistical significance calculated by Tukey-Kramer test: $*P < 0.05$. (**C**) Expression levels of PrP^{C} in the brain of uninfected mice. A brain sample, equivalent to 50 μg in wet weight, was loaded in each lane.

Figure 5. Activation of complement systems. Western blot analysis of C1qa in the brain of uninfected mice and Chandler- or Fukuoka-1-inoculated mice. C1qa accumulated only in the prion-infected animals regardless of the mouse genotype or prion strain. A brain sample, equivalent to 1 mg in wet weight, was loaded in each lane.

Figure 6. Flotation assay of lipid raft-associated proteins. Floating patterns of a GPI-anchored complement-regulatory molecule CD55 (**A**), a lipid raft marker flotillin 1 (**B**), PrP (**C**), a GPI-anchored PrP-associated calcium channel protein CACNA2D1 (**D**), and a GPI-anchored protein Thy1 (**E**) in fractions separated by Optiprep density gradient centrifugation were examined using brain homogenates of uninfected mice. Flotillin 1 and PrP dispersed from the lipid raft fractions (fractions 7-11) to the non-raft fractions (fractions 15-18) in GD2/GM2 KO mice. Data are representative of assays repeated independently three times.

522

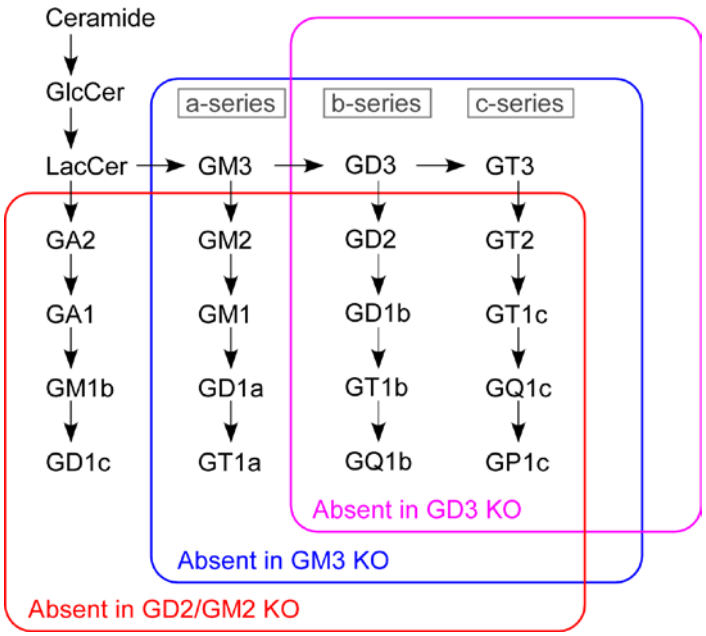
Ceramide
GlcCer
LacCer
GA2
GA1
GM1b
GD1c
a-series
b-series
c-series
GM3
GD3
GT3
GM2
GD2
GT2
GM1
GD1b
GT1c
GD1a
GT1b
GQ1c
GT1a
GQ1b
GP1c
Absent in GD3 KO
Absent in GM3 KO
Absent in GD2/GM2 KO

Figure 1

523

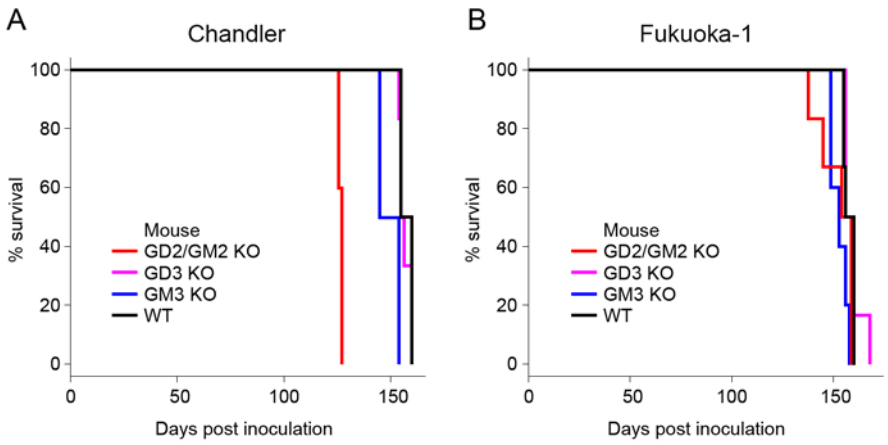
A
Chandler
100
80
60
40
20
0
% survival
Mouse
GD2/GM2 KO
GD3 KO
GM3 KO
WT
0
50
100
150
Days post inoculation
B
Fukuoka-1
100
80
60
40
20
0
% survival
Mouse
GD2/GM2 KO
GD3 KO
GM3 KO
WT
0
50
100
150
Days post inoculation

Figure 2

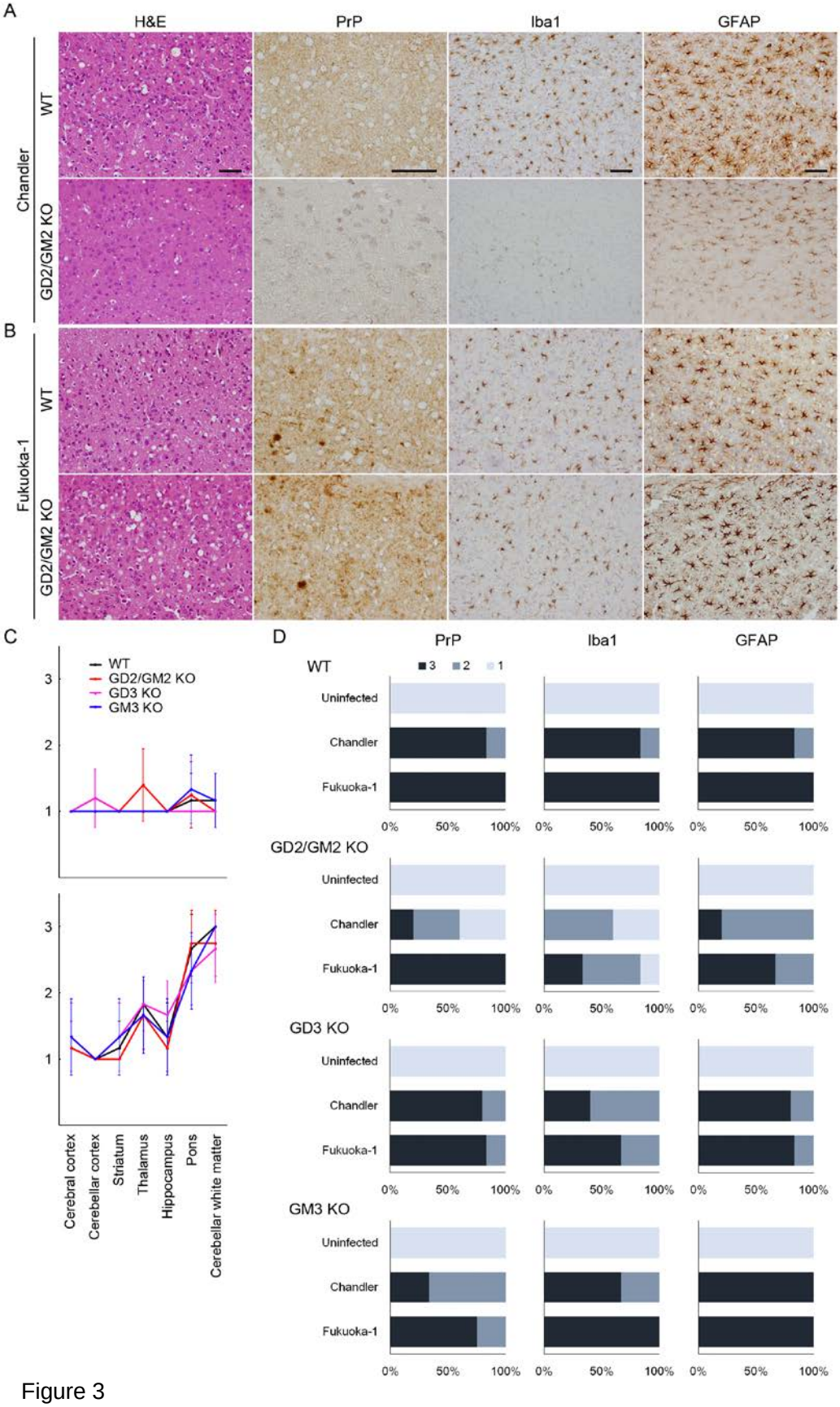
A
H&E
PrP
Iba1
GFAP
Chandler
WT
GD2/GM2 KO
B
Fukuoka-1
WT
GD2/GM2 KO
C
WT
GD2/GM2 KO
GD3 KO
GM3 KO
3
2
1
Cerebral cortex
Cerebellar cortex
Striatum
Thalamus
Hippocampus
Pons
Cerebellar white matter
D
PrP
Iba1
GFAP
WT
3
2
1
Uninfected
Chandler
Fukuoka-1
0%
50%
100%
GD2/GM2 KO
GD3 KO
GM3 KO

Figure 3

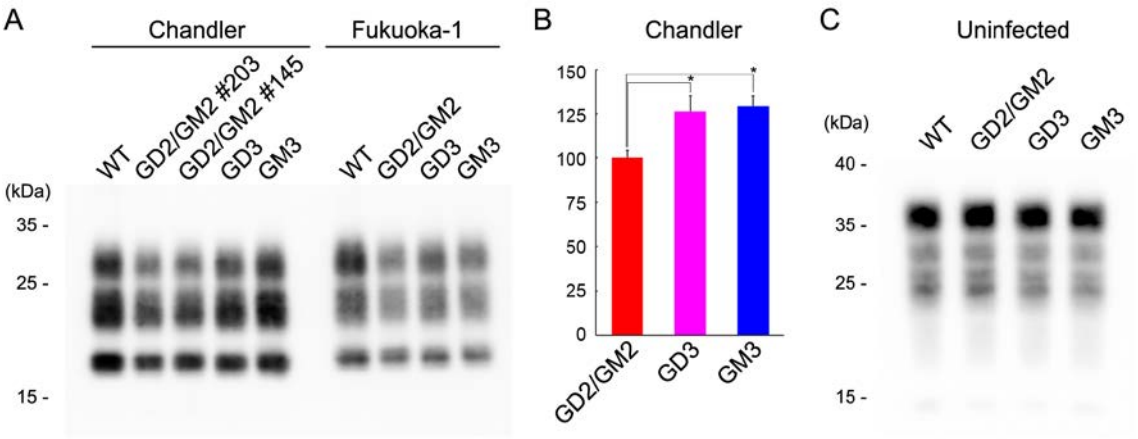
A
Chandler
Fukuoka-1
WT
GD2/GM2 #203
GD2/GM2 #145
GD3
GM3
WT
GD2/GM2
GD3
GM3
(kDa)
35 -
25 -
15 -
B
Chandler
150
125
100
75
50
25
0
GD2/GM2
GD3
GM3
C
Uninfected
(kDa)
WT
GD2/GM2
GD3
GM3
40 -
35 -
25 -
15 -

Figure 4

526

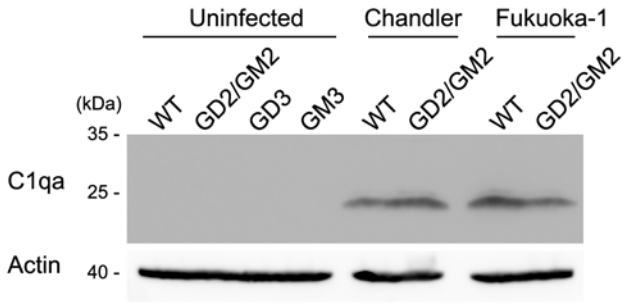
Uninfected
Chandler
Fukuoka-1
(kDa)
WT
GD2/GM2
GD3
GM3
WT
GD2/GM2
WT
GD2/GM2
35 -
25 -
40 -
C1qa
Actin

Figure 5

527

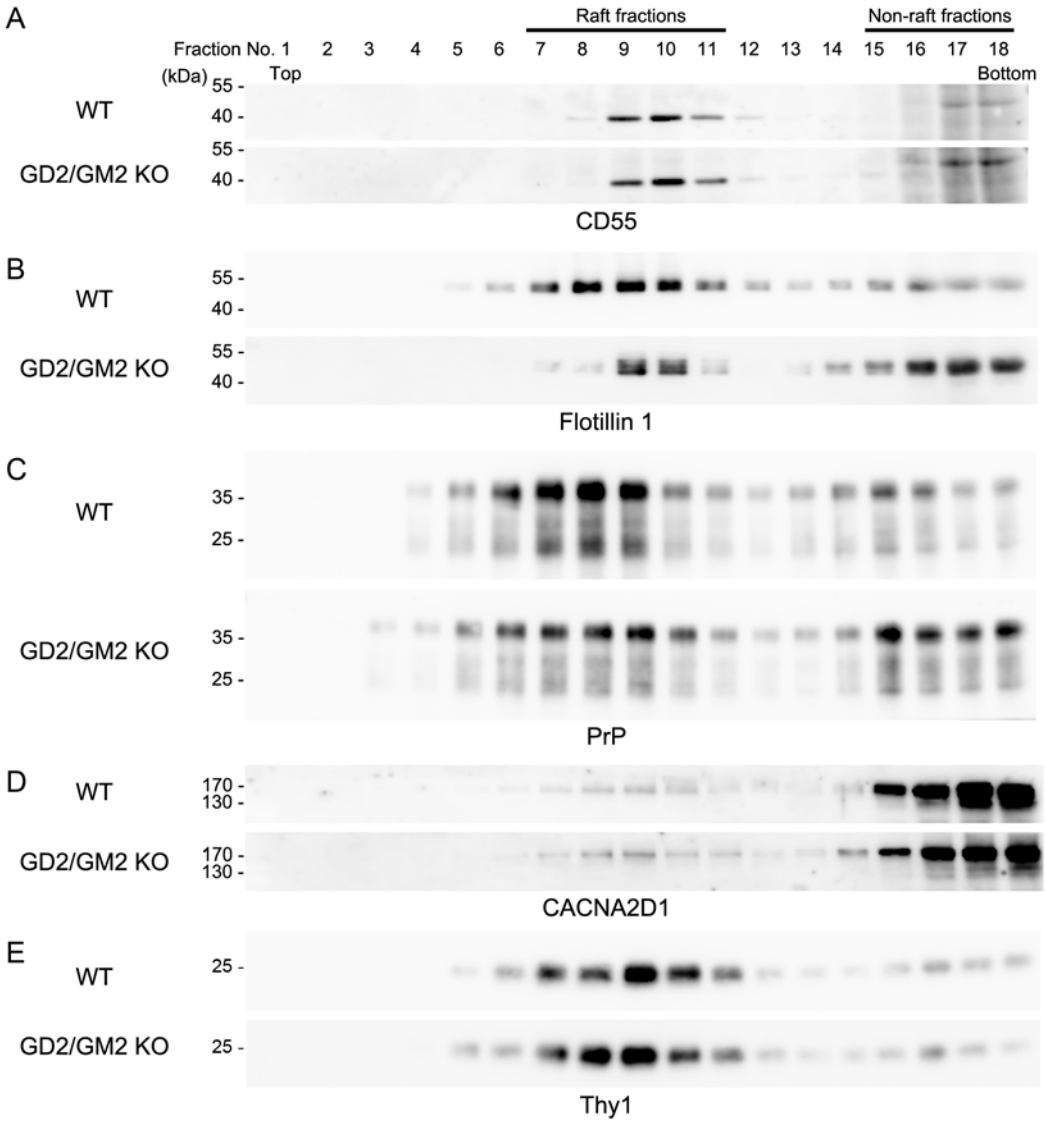
A
Raft fractions
Non-raft fractions
Fraction No. 1 2 3 4 5 6 7 8 9 10 11 12 13 14 15 16 17 18
(kDa)
Top
Bottom
WT
GD2/GM2 KO
55 -
40 -
CD55
B
Flotillin 1
C
35 -
25 -
PrP
D
170 -
130 -
CACNA2D1
E
Thy1

Figure 6